Nanomechanical properties of single amyloid fibrils

2012 J. Phys.: Condens. Matter 24 243101

(http://iopscience.iop.org/0953-8984/24/24/243101)

J. Phys.: Condens. Matter **24** (2012) 243101 (12pp) doi:10.1088/0953-8984/24/24/243101

TOPICAL REVIEW

Nanomechanical properties of single amyloid fibrils

K K M Sweers[1], M L Bennink[1] and V Subramaniam[1,2]

[1] Nanobiophysics, MESA+ Institute for Nanotechnology, Faculty of Science and Technology, University of Twente, Enschede, The Netherlands
[2] Nanobiophysics, MIRA Institute for Biomedical Technology and Technical Medicine, Faculty of Science and Technology, University of Twente, Enschede, The Netherlands

E-mail: k.k.m.sweers@utwente.nl, m.l.bennink@utwente.nl and v.subramaniam@utwente.nl

Received 9 February 2012, in final form 20 April 2012
Published 15 May 2012
Online at stacks.iop.org/JPhysCM/24/243101

Abstract

Amyloid fibrils are traditionally associated with neurodegenerative diseases like Alzheimer's disease, Parkinson's disease or Creutzfeldt–Jakob disease. However, the ability to form amyloid fibrils appears to be a more generic property of proteins. While disease-related, or pathological, amyloid fibrils are relevant for understanding the pathology and course of the disease, functional amyloids are involved, for example, in the exceptionally strong adhesive properties of natural adhesives. Amyloid fibrils are thus becoming increasingly interesting as versatile nanobiomaterials for applications in biotechnology.

In the last decade a number of studies have reported on the intriguing mechanical characteristics of amyloid fibrils. In most of these studies atomic force microscopy (AFM) and atomic force spectroscopy play a central role. AFM techniques make it possible to probe, at nanometer length scales, and with exquisite control over the applied forces, biological samples in different environmental conditions.

In this review we describe the different AFM techniques used for probing mechanical properties of single amyloid fibrils on the nanoscale. An overview is given of the existing mechanical studies on amyloid. We discuss the difficulties encountered with respect to the small fibril sizes and polymorphic behavior of amyloid fibrils. In particular, the different conformational packing of monomers within the fibrils leads to a heterogeneity in mechanical properties. We conclude with a brief outlook on how our knowledge of these mechanical properties of the amyloid fibrils can be exploited in the construction of nanomaterials from amyloid fibrils.

(Some figures may appear in colour only in the online journal)

Contents

1. Introduction

The term amyloid fibril was first introduced in 1854 and is usually associated with neurodegenerative diseases like Alzheimer's disease, Parkinson's disease or Creutzfeldt–Jakob disease [1, 2]. More recently, the ability to form amyloid fibrils was found to be a generic property of proteins [3, 4]. Indeed, common food proteins, like β-lactoglobulin or ovalbumin, have the ability to form amyloid fibrils [5, 6]. Amyloid is a general term for protein aggregates with the following three characteristics: (1) the fibrils are around 10 nm in diameter, (2) they bind to dyes such as thioflavin *T*, and (3) the fibrils consist of cross β-strands stacked perpendicular to the fibril axis exhibiting intermolecular hydrogen bonds [1, 2, 7–9].

Disease-related amyloid fibrils are relevant for understanding the pathology, origin and progression of the disease. Moreover, amyloid fibrils, whether formed from disease-related or other proteins, are becoming increasingly interesting for applications in nanobiotechnology [10]. Most studies so far have focused on the morphological properties of the amyloid fibrils such as fibril length and fibril height, using technologies such as atomic force microscopy (AFM) imaging or transmission electron microscopy. Other studies have addressed the twisting characteristics of amyloid fibrils [11, 12]. Nuclear magnetic resonance or x-ray diffraction methods have been used to investigate the packing and assembly of monomer units within amyloid fibrils [8, 13, 14]. Despite a rather large body of literature (reviewed, for example, in Gosal *et al* [15]) a number of open questions remain regarding the structure of amyloid fibrils.

One particular characteristic observed with many amyloid fibrils, and which severely complicates the interpretation of the studies, is polymorphism. Polymorphism refers to the tendency of amyloid-forming proteins to form a variety of fibrils all having different structural characteristics [16–18]. An alternative method to shed some light on these open questions is to study the mechanical properties of these nanostructures. Mechanical properties of fibrils are often directly linked to the structure. This relation makes it possible to retrieve, from mechanical characteristics, information on the shape and packing of the individual monomers within a fibril.

In the last decade a vast number of studies have reported on obtaining the mechanical characteristics of amyloid fibrils. Understanding the mechanical characteristics of disease-related amyloid fibrils may yield an insight into the formation and structure of amyloid nanostructures, and eventually into the mechanisms of cellular toxicity. Amyloid fibrils are found to be stiffer than cytoskeleton components such as actin filaments (1.8 GPa) [19, 20], microtubules (600 MPa) [21, 22], or intermediate filaments (6.4 MPa) [23]. So although the fibrils themselves often appear not to be toxic compared to the intermediate oligomeric aggregation states, the mechanical properties of amyloid fibrils could interfere with cytoskeletal dynamics. The modulus of elasticity values of amyloid fibrils are in the range of collagen fibrils (1–5 GPa) [24, 25], which suggest that in the extracellular space (where, for example, Aβ fibrils are found), these fibrils could have fewer mechanical consequences for cell motility.

Amyloid fibrils are also increasingly found naturally in functional roles. Recently, over 30 human peptide hormones were found that are stored in amyloid-type granules for long-term use [26]. This could be translated into a system to overcome the short-term delivery problems of drugs by using amyloid as a controlled drug release system [27]. Bacteria, like *Salmonella* and *Escherichia coli,*, and algae use functional amyloid to modulate surface adhesion [28, 29]. The interest in mechanical properties for these kinds of amyloids is mainly in their adhesive properties. Sullan *et al* studied the adhesive properties of polymerized barnacle glue, consisting also of amyloid, which is a large contributor to the fouled areas on marine ship hulls [30]. Deeper insights into the specific mechanical properties of amyloid could be used to create new surfaces with a monolayer of amyloid fibrils with specific adhesive properties.

Due to the self-assembly property of amyloid fibrils, these nanostructures are also interesting as templates to create filaments of other materials that do not have this capability. Many protein peptides can be functionalized with, for instance, fluorescent dyes or metal nanoparticles to create functionalized wires. For instance, Scheibel *et al* covalently linked gold particles to fibrils formed by a modified NM Sup35 (*N*-terminal and middle region of yeast prion Sup35) peptide. These coated fibrils displayed conductive properties [31]. Also diphenylalanine fibrils are of interest for this purpose. Because of the hollow core, these fibrils can be functionalized inside and outside creating a coaxial type nanowire [32]. Aside from the light and electron transport properties, the need to know mechanical characteristics is important when these nanowires are used in the construction of larger light-harvesting complexes or nano-electronics.

AFM and atomic force spectroscopy play a central role in most existing studies of mechanical properties of amyloid fibrils. AFM allows probing biological samples with very low and controlled forces in different environmental conditions. Three different approaches can be distinguished (figure 1). The first approach is nanoindentation, where the AFM tip acts as an indenter. The modulus of elasticity can be extracted from the force–displacement curve using elastic contact models. The second approach involves bending experiments in which the amyloid fibril is suspended over a channel and the AFM tip is used to bend the fibril. In the third and last method, amyloid fibrils are deposited on a surface after which they are imaged. From these images the bending rigidity can be determined by analyzing the curvature of the individual fibrils using statistical mechanical theory of semi-flexible polymers, for instance with end-to-end distances.

In this review we first briefly introduce the different AFM-based methods for probing mechanical properties of single amyloid fibrils. We give an overview of the existing studies, in relation to all the different challenges (like small size, anisotropy and heterogeneity) associated with these AFM-based mechanical studies of nanoscale fibrils.

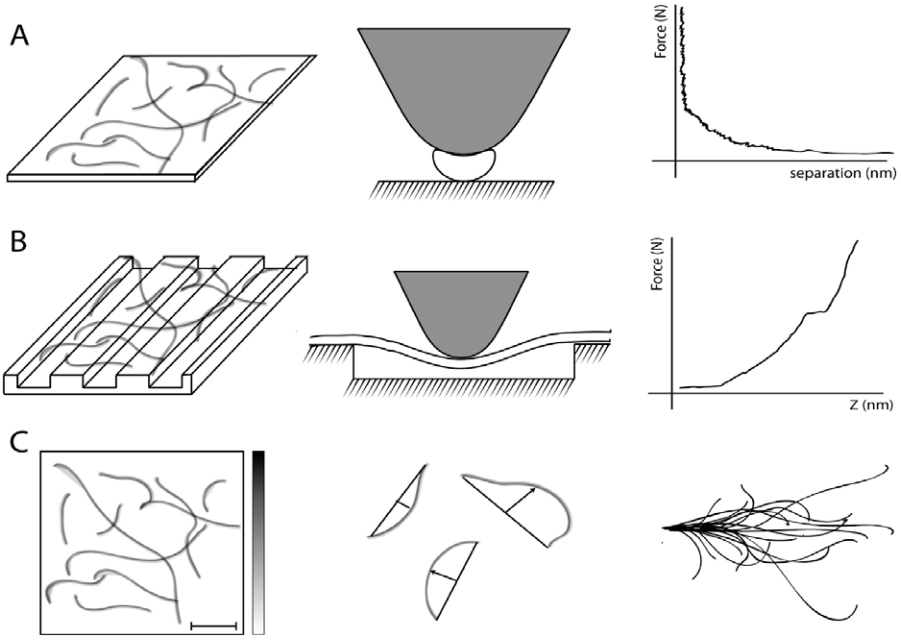

Figure 1. Overview of three different AFM-based methods to measure mechanical properties of single fibrils. Panel (A) depicts the AFM-based nanoindentation to probe for spring constants or stiffness values with nanometer-scale spatial localization. The tip acts as an indenter and pushes into the fibril. This results in a force–distance curve that can be analyzed for elastic properties. Panel (B) shows bending experiments, which use the same AFM configuration as for nanoindentation, only the fibrils are suspended on channels to determine the modulus of elasticity along the fibril axis. The force curve displays the elastic properties and eventually a breaking point. (C) Here the fibril mechanical properties are derived from the 2D AFM images of the individual fibrils. The fibrils are traced and a contour of each fibril is generated. From the curvature of the contour, the bending rigidity of the fibril can be calculated using statistical mechanical theory of semi-flexible polymers by determining the distance between the midpoint of the fibril to the straight rod ground state. Comparing groups of fibril contours formed by different proteins could already shed light on different mechanical properties.

2. Methods for probing nanomechanical properties of amyloid fibrils

In 1986 the first atomic force microscope was realized as a variant of the scanning tunneling microscope [33, 34]. In AFM a 3D reconstruction of the sample topography is made by scanning the sample. The sample is moved in x, y and z directions with respect to the AFM tip, sample-scanning method, or vice versa in a tip-scanning set up. The AFM tip is at the end of a leaf spring or cantilever that bends according to the sample topography and interaction forces (like short-range van der Waals forces or long-range electrostatic forces). This bending of the cantilever, and thus interaction between tip and sample, is monitored with a laser beam reflected from the back of the cantilever onto a position sensitive photodiode. Since the AFM is a force-measuring technique, it is not only an excellent technique for analyzing morphological parameters by creating 3D topography maps, but is also very suitable for determining mechanical characteristics which can provide additional insights into the structure and assembly of amyloid fibrils.

2.1. Nanoindentation

Nanoindentation on the AFM is done by atomic force spectroscopy where the ability of the AFM to precisely measure the interaction forces between the tip and sample is used. In nanoindentation mode the AFM tip approaches and is pushed into the sample until a predefined force is reached; at this point the tip is retracted again. During this complete cycle the position of the tip as well as the force exerted on the cantilever are accurately monitored, resulting in a force–distance curve (figure 2). For most biological samples, the AFM tip acts as a stiff indenter, and can therefore be used to measure the mechanical properties of the sample. The stiffness of the sample can be extracted from the part of the curve where the tip is in contact with the sample (figure 2).

2.1.1. Contact mechanics models. Contact mechanics models are needed to relate the stiffness extracted from the force curves to an actual modulus of elasticity. There are several contact models to analyze force curves generated by a nanoindentation experiment. We will briefly discuss here three models, namely the Hertz, Johnson–Kendall–Roberts (JKR) and Derjaguin–Muller–Toporov (DMT) models, which are mathematically represented as:

$$\begin{aligned} &\text{Hertz}: \ F = \tfrac{4}{3}E^*\sqrt{R}\delta^{3/2} \\ &\text{DMT}: \ F = \tfrac{4}{3}E^*\sqrt{R}\delta^{3/2} - 2\pi R\gamma \\ &\text{JKR}: \ F = \tfrac{9}{4}E^*\sqrt{R}\delta^{3/2}\Delta\gamma\pi \\ &\frac{1}{E^*} = \frac{1-\upsilon_{\mathrm{m}}^2}{E_{\mathrm{m}}} + \frac{1-\upsilon_{\mathrm{i}}^2}{E_{\mathrm{i}}} \end{aligned} \qquad (1)$$

where F is force, δ is indentation, R tip radius, E^* the reduced elastic modulus and γ the work of adhesion, defined as in equation (1), The reduced elastic modulus is comprised of

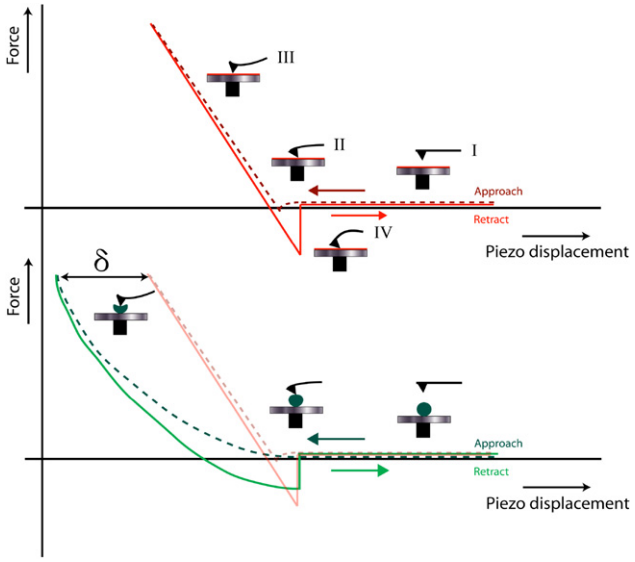

Figure 2. Typical approach and retract curve. Different regions are highlighted: where the tip is above the sample (I), the tip snaps in onto the sample due to van der Waals forces (II), the tip presses on the sample leading to cantilever deflection (III), and finally, when the tip is retracted again, the tip sticks to the sample due to adhesion forces before finally snapping free (IV). The small difference between the approach and retract curve is called contact hysteresis which is caused by friction effects between the tip and the sample [35]. The red curve indicates a force–distance curve on a hard reference sample and the green curve represents indentation on a soft sample. The difference δ between both curves is the indentation.

the modulus of elasticity and Poisson ratio of the material to be indented, E_m and ν_m, and the modulus of elasticity and Poisson ratio of the indenter, E_i and ν_i, here the AFM tip. Ideally, the indenter has an infinite modulus of elasticity and a low Poisson ratio, which renders the second term zero.

The Hertz model assumes a non-adhesive contact between two contacting bodies. In case there is adhesion between the two bodies, the JKR and DMT models are most often used for the interpretation of nanoindentation data. The DMT model assumes the contact area between the tip and the material as in the Hertz model, but includes an additional constant adhesion term, representing adhesive forces outside the contact area. This means that the contact profile remains the same but an additional adhesive force is added outside the area of contact, so the curve is identical to that of the Hertz model with an offset (adhesion) in force. In contrast to the DMT model, the JKR model assumes adhesion inside the area of contact [36–38].

In order to determine the elasticity modulus, irrespective of the model used, the contact area must be determined. In the equations above, the contact area is calculated assuming a spherical tip with radius R, assuming the contact to be modeled by that of a sphere touching an infinitely large plane. Since the diameter of a typical amyloid fiber is about 10 nm, which is about the same order of magnitude as the tip radius, this condition is not valid. Using an equivalent tip radius in the above equations can compensate for this point. The equivalent tip radius, R_e, is defined by equation (2), in which the AFM tip is assumed to be a sphere with radius R_t indenting an infinitely long cylinder, that represents the fibril, with radius R_f:

$$R_e = \sqrt{\frac{(R_t^2 R_f)}{(R_t + R_f)}}. \quad (2)$$

2.1.2. Surface property mapping techniques. As explained in section 2.1.1, nanoindentation can be performed at one specific point of the sample in order to locally probe the mechanical properties with nanometer resolution. It is also possible to perform nanoindentation in a raster pattern such that mechanical properties, like modulus of elasticity, adhesion or energy dissipation are determined for each pixel of a surface. This mode is known as the force–volume mode and creates a set of images for all parameters [39]. The force–volume mode is very helpful in mapping the heterogeneous properties of amyloid fibrils. However, with each individual nanoindentation experiment taking about 1 s, this method can be very time consuming. Recently novel methods have been developed to probe for mechanical properties at much higher speeds, which significantly decrease the imaging time [40–42]. Examples of such methods are harmonic force microscopy, pulsed force microscopy or PeakForce quantitative nanomechanical (QNM). PeakForce QNM is an imaging mode in which the cantilever is oscillated at a frequency of 1 kHz, with each oscillation resulting in a single force–distance curve. From this force–distance curve elastic parameters can be extracted. The feedback is applied on the maximum force that is applied to the sample, ensuring the sample is probed with the same force at each position. HarmoniX is based on the nonlinear dynamic behavior of a cantilever in tapping mode due to repulsive and attractive forces caused by the specific material characteristics of the sample acting on the tip [43, 44]. By using cantilevers on which the tip is positioned off-center, the interaction between the tip and sample also induces a torsional mode. This torsional mode acts as a high bandwidth force sensor in which all the higher harmonic signals from the vertical deflection can be measured. From this a force–distance curve can be reconstructed, and mechanical properties can be extracted.

2.1.3. Single molecule spectroscopy. One aspect that has not been extensively discussed above is the use of atomic force spectroscopy for single molecule pulling. Single molecule force spectroscopy is frequently used to determine the fold of single proteins and peptides, see for reviews [45, 46]. Force curves can predict whether amino acid chains are folded, for instance in β-sheet conformation or unstructured. Further, the persistence length of amino acid chains can be determined. Although, this approach does not yield results on the mechanical properties of full-length assembled amyloid fibrils, it can be applied to provide insight into the intermolecular forces involved in fibril assembly, and possibly the folding transition it undergoes as a protein monomer is assembled into the fibril structure.

In the context of amyloid fibrils, when the AFM tip is specifically or aspecifically bound to individual monomers within the fibril, these monomers can be pulled

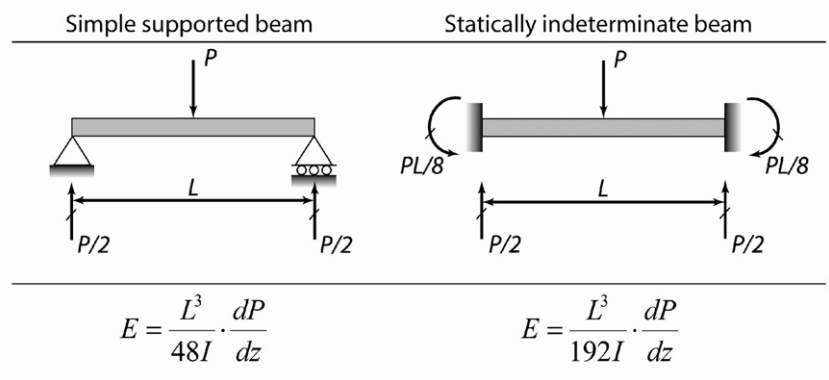

Figure 3. Supported beam models for AFM bending experiments. A simple supported beam with at one side a pin support and at the other a roller support (left) and a statically indeterminate beam fixed at both ends (right), with the corresponding formulas for modulus of elasticity.

out of the fibril. This nanoscale pulling experiment gives a force–distance curve, potentially with different steps that could indicate β-sheet unzipping, and eventually lead to a final rupture force [28, 47].

2.2. Single filament bending experiments

AFM-based nanoindentation only probes very local mechanical properties by exerting a force in a direction perpendicular to the amyloid fibril axis. Amyloid fibrils, however, have an anisotropic structure and are therefore expected to display anisotropic mechanical properties. To study the mechanical properties along the fibril axis a different type of experiment must be performed, for example, a bending experiment. Here, an individual amyloid fibril is suspended over a micro- or nanometer sized channel and the AFM is used to accurately measure the force needed to bend the freely suspended part of the fibril.

Nanoscale fibrils that are supported over channels can be modeled as a simple supported beam in which the force from the AFM tip is assumed to be a single-point load P in the middle of the beam. Depending on the boundary conditions, there are two models that can be used (figure 3). The first model is that of a simple supported beam. As the load is applied to the beam, the beam can bend and freely rotate on the points where it is supported. However, amyloid fibrils are known for their strong adhesive properties suggesting that this boundary condition is probably not valid. The second model is that of a statically indeterminate beam, where both ends of the beam are fixed. Assuming that the amyloid fibril is firmly attached to the edges of channels, this boundary condition would be the appropriate one.

These two models are used for larger filaments like collagen [24], *para*-hexaphenylene nanofibers [48] or elastic fibers [49]. In these experiments typical channel widths were in the 1–10 μm range. For filament sizes that are larger than the AFM tip, as is the case for collagen fibers, it is valid to consider the size of the contact area as a point load. However, for amyloid fibrils, which are small compared to the AFM tip size, and are to be bent over much smaller channels (range of 50–200 nm), the size of the contact area can no longer be considered a point load. This load becomes a distributed load that is dependent on the tip size and shape. Obtaining a mathematical representation for this distributed load depending on the tip shape and the small interaction forces that are involved can be challenging.

2.3. Statistical analysis of thermal fluctuations

As mentioned above, bending experiments are very challenging for amyloid fibrils both from an experimental point of view and in the analysis and interpretation of the data. Another way that the elastic properties of amyloid fibrils reveal themselves is through the shape of the fibrils, and in particular by the curvature they exhibit when in solution or on a surface. By making topography images of these fibrils using either contact or tapping mode AFM, the fibril contours can be traced either manually or by using a tracing algorithm. From these traces it is possible to determine the end-to-end distance of a fibril, and its curvature or the deviation from a straight segment. Using statistical mechanical theory of semi-flexible polymers, it is possible to derive the bending rigidity or flexural rigidity of the amyloid fibril. This bending rigidity is proportional to the persistence length of a filament, which is the length of a filament over which thermal bending becomes appreciable.

There are several approaches to measure persistence length or bending rigidity. For instance, the end-to-end distance can be measured. When any bending has occurred, this length is always smaller than the contour length of the filament. When the contour length of the filament is much smaller than the persistence length (L_p), the persistence length can be estimated by the fluctuations in shape [50]. This method is often used in the case of amyloid fibrils. The bending rigidity (κ) of the semi-flexible amyloid fibrils can be derived from the average magnitude of the thermally induced shape deviations from a straight line connecting the end points [51–53] according to the following equations:

$$k_B T \frac{L^3}{48\langle v(x)^2\rangle} \leq \kappa \leq k_B T \frac{L^3}{24\langle v(x)^2\rangle} \tag{3}$$

where k_B is the Boltzmann constant, T the temperature in Kelvin, L the contour length of the fibril segment and $v(x)$

is the distance from the midpoint of the fibril segment to the secant line of the fibril segment. Equation (3) provides two outer limits for the bending rigidity, representing a situation in which the fibrils are irreversibly trapped when deposited onto the surface and a situation in which the fibrils are thermally equilibrated on the surface before they adhere more strongly.

One important aspect of these calculations is the choice of fibrils in the 2D image. One should only choose filaments which do not cross other filaments or particles on the surface. Crossing other fibrils or particles could affect fluctuations of the fibrils and influence the shape of the fibril contour, subsequently affecting the results of the analysis.

3. Mechanical properties of amyloid fibrils

The number of mechanical studies on amyloid fibrils probed with AFM is rapidly increasing. These studies report on bending rigidities, moduli of elasticity, stiffness, and rupture forces of individual monomers within the fibrils, and often link these properties to structural information.

When determining mechanical properties with an AFM, all possible approaches are accompanied by their own specific calibration issues. Most important is the cantilever choice and cantilever stiffness calibration. For nanoindentation, the highest sensitivity is achieved if the spring constant of the cantilever is in the same range as the spring constant of the sample. The calibration of this spring constant can be done using the thermal noise method, which has associated errors of around 5%, or response methods like the added mass method (10%–20% error) [54–56]. Furthermore, for all calibration methods the deflection sensitivity is needed, which also gives rise to a small error of 2% [55]. The accuracy of determining the tip radius can also influence the results greatly. All these issues have been described previously [56]. The only method that is relatively insensitive to these calibration issues is the bending rigidity determination approach, although this method also relies on assumptions like whether the samples are able to thermally equilibrate on the surface.

In addition to the experimental considerations mentioned above, specific structural characteristics of amyloid fibrils, such as size, polymorphism, and anisotropy, influence the mechanical properties of amyloid fibrils. In the next section we focus on the consequences of these parameters and of environmental conditions on the accurate determination of amyloid mechanical properties.

3.1. Amyloid fibril size

One of the most significant challenges of performing nanoindentation experiments on amyloid fibrils is the small diameter (∼10 nm) of these fibrils. Firstly, the area of contact used in the elastic contact models (equation (2)) is only correct if the indentation takes place precisely on top of the amyloid fibril. An accurate *XY*-feedback system is needed to precisely position the tip above the fibril. If this is not done correctly, the measurements will give incorrect results, as we have recently shown in a study using HarmoniX, which revealed an increased modulus of elasticity near the edges

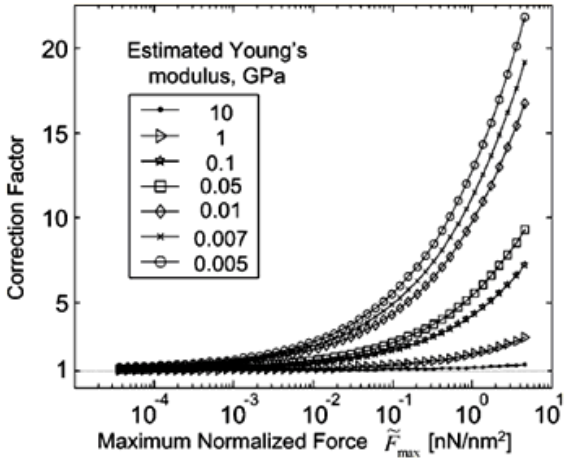

Figure 4. Correction factors for the finite sample thickness effect. The graphs show the dependence of the correction factors on the maximum normalized force. The correction factors were calculated for several samples with different Young's moduli. An apparent value of the Young's modulus for each line is indicated in the inset. Reproduced with permission from [58]. Copyright 2006 American Chemical Society.

of fibrils [56]. Secondly, when performing nanoindentation measurements on these nanoscaled structures, whether by means of single-point experiments or the newly introduced surface property mapping techniques, an important issue to consider is the effect of finite sample thickness. These effects come into play when the sample starts to compress and the AFM cantilever 'feels' not only the sample but also the underlying substrate up to a point where the sample is completely compressed and only the substrate accounts for the signal. In the initial 20% of the total height of a sample these effects are thought to be negligible when the sample is relatively large compared to the tip [30]. However, when indenting amyloid fibrils, this 20% value is only ∼2–3 nm, which makes it more difficult to analyze the indentation curves. The AFM tip is approximately the same size as or larger than the fibril. It is difficult to indicate the precise point of contact and indeed to determine whether actual contact has occurred or if the signal measured is only due to long-range repulsive or attractive forces. Akhremitchev *et al* have developed a correction factor depending on the sample size, sample modulus of elasticity and the maximum applied force (figure 4) [57].

Guo *et al* used this method to correct for finite sample thickness effects while determining the modulus of elasticity of insulin fibrils, which decreased the elastic modulus one order of magnitude from 141 MPa to only 14 MPa after correction [58]. Others also adopted this correction method, for instance when measuring the modulus of elasticity of different types of poly(ValGlyGLyLeuGly) fibrils (3.7–7.1 MPa) and bovine elastin fibrils (1.1 MPa) [59]. Here the correction factor was ∼4–5 due to the softness of the sample; however, also stiffer amyloid fibrils made of the protein α-synuclein did show a small decrease in the modulus of elasticity after correction for finite sample thickness effects to 1.3 GPa (correction factor ∼ 1.3) [56].

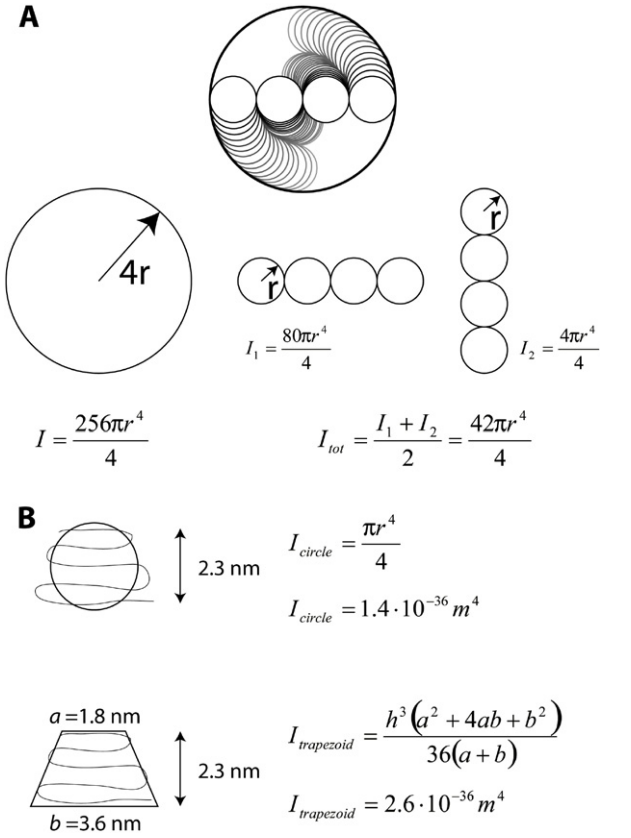

Figure 5. Examples of cross-sections of amyloid fibrils with their corresponding second moments of inertia. (A) Difference between moments of inertia when a fibril is assumed to be a circular rod or consists of four lateral associated filaments that twist results in a roughly six-fold difference in moment of inertia. (B) Shape of α-synuclein monomer with five β-strands increasing in size [13]. A circular shape reduces the moment of inertia roughly two-fold when the same dimensions, like a monomer height of 2.3 nm, are used as for a trapezoid shape.

The bending experiments are also challenging for these small length scale fibrils. As discussed in the instrumental section, the load applied on the fibril is probably not a point load but a distributed load that is challenging to model. Also the channel size plays a role; when a fibril is rather flexible or the channel is very wide, it is often easy for adsorption forces to pull the fibril into the channel. We attempted several channel patterned surfaces for this purpose and often observed fibrils which were aligned with the channels or, when they crossed the channels, were completely sunken in to the channels. When the fibril completely sinks into the channel, or follows the contours of the channel, it is no longer possible to perform the bending experiments. Successful bending experiments on insulin fibrils have been performed on a gold patterned surface with channels between 50 and 100 nm [53]; these surfaces are not commonly available and require special fabrication using advanced strategies.

3.2. Amyloid fibril structure

The ultrastructure of amyloid fibrils also plays a significant role in determining the modulus of elasticity. For the bending experiments and bending rigidity method the moment of inertia is required to determine the modulus of elasticity. This moment of inertia is dependent on the cross-sectional area of a fibril. Amyloid fibrils display a large degree of polymorphism, or variation in their morphologies. Earlier studies suggested that the hierarchically twisted filament model could be a generic model for all amyloid [60]. However, recently twisted, laterally associated filaments have also been reported for β-lactoglobulin amyloid fibrils. These fibrils show increasing persistence lengths when the number of filaments increases, from 1 μm for a single filament to almost 4 μm for five filaments [61]. The packing of filaments within a fibril could account for a large difference in results. Adamcik *et al* already described a linear dependence of the moment of inertia on fibril height when the number of filaments increases. In figure 5(A) we show an example of a six-fold difference between moments of inertia when a fibril is assumed to be a circular rod or consists of four laterally associated filaments which twist. Aside from the packing, the conformation of the monomer also plays a role. For simplicity many studies use a circular conformation for the moment of inertia [24, 49, 53, 61]. However, β-sheet folded proteins are probably not circular. For α-synuclein the fold is believed to be trapezoid shaped [13]. A roughly two-fold change in moment of inertia is found depending on whether the primary sequence of the monomer is assumed to follow this trapezoid shape or a circular shape (figure 5(B)) [13, 62].

Several studies have demonstrated that amyloid fibrils can demonstrate significant variations in morphologies (polymorphism), see for reviews [16–18, 63]. Aβ_{1-40} fibrils for instance, show both twisted fibrils and laterally associated filaments depending on the aggregation conditions [11]. However, morphological differences can also lead to differences in mechanical characteristics. Aβ fibrils comprised of different peptide length monomers give different fibrils with different rupture forces [64, 65]. Fibrils comprised of α-synuclein can lead to curly fibrils with a persistence length of 0.17 μm after several filtration-like steps during aggregation or, when the aggregation is not interfered with, to straight fibrils with persistence lengths of up to 140 μm [66]. β-lactoglobulin fibrils aggregated with or without the presence of ethanol also exhibit very different persistence lengths (2.3 μm versus 0.003 μm respectively) [67]. Also, β-lactoglobulin fibrils made with different agitation methods lead not only to morphological differences, but also differences in rupture forces measured by single molecule force spectroscopy [68].

Sometimes, one aggregation reaction produces multiple fibril species. These fibril species can have similar mechanical properties, like periodic and non-periodic α-synuclein fibrils that display the same bending rigidity values of around 1.5×10^{-24} N m^2 [62]. However, protofibrils formed by HypF-*N* did show two populations with different bending rigidities of $2.9 \pm 0.1 \times 10^{-28}$ and $4.2 \pm 0.4 \times 10^{-29}$ N m^2 with no distinct morphological differences. This observation indicates that mechanically different protofibrils can exist, each of which could further exhibit differences in aggregation tendencies [69].

3.3. Amyloid fibril heterogeneity and anisotropy

The twisted morphological feature of amyloid fibrils, already discussed above, could lead to anisotropic and heterogeneous characteristics in the mechanical properties. For collagen fibrils it has already been shown that the ribbon-like morphological characteristics also display an almost two-fold difference in modulus of elasticity (1.2 GPa for the gap region and 2.2 GPa for the higher overlap region) [70]. Simple AFM contact mode sideways scratching of α-synuclein fibrils on a surface already revealed that twisted fibrils were weaker at the twist sections [71]. Nanoindentation on glucagon fibrils also revealed different moduli of elasticity at different sections along the twist. The corresponding force–volume images showed that the fibril peaks were more compliant compared to the troughs [72]. The recently introduced high-speed surface property mapping techniques facilitate the analysis of heterogeneous features. However, first results with Peakforce and HarmoniX did not reveal differences along the twist of α-synuclein fibrils [56]. Also, peakforce tapping on β-lactoglobulin did not reveal differences along the twist that were not induced by the underlying substrate [73]. Mechanical anisotropy of amyloid fibrils refers to a difference in mechanical properties when measured either radially or axially. Nanoindentation probes for mechanical properties perpendicular to the fibril axis, while bending experiments yield values for the axial direction. For insulin fibrils the nanoindentation measurements resulted in values with an average of 14 MPa [58] while bending experiments or bending rigidity measurements from 2D images resulted in values up to 3.3 and 6.3 GPa respectively [53]. Nanotubes formed by the diphenylalanine peptide display similar differences between the axial modulus of elasticity compared to the elasticity measured radially. However, this difference was less pronounced compared to insulin. Nanoindentation measurements resulted in a spring constant of 160 N m^{-1} for the tubes which was calculated with finite element analysis to correspond to a modulus of elasticity of $\sim$19 GPa [74]. However, bending experiments on similar tubes gave an average modulus of elasticity of 27 $\pm$ 0.4 GPa [75]. A study of poly(ValGlyGlyLeuGly) fibrils freely suspended over two underlying fibrils for bending experiments and indentation studies on the same fibril resting on the surface also showed a difference in axial stiffness compared to the radial stiffness [76].

3.4. Environmental conditions

Environmental conditions are often of importance in AFM studies. Morphological features like size and periodicity already appear to change upon drying or when using different scanning buffers [12, 77]. The high modulus of elasticity values for amyloid fibrils compared to other biological materials, for example dragline silk, which has values up to 10 GPa [78], already indicate a tight, densely packed, fibril core. This suggests that one could expect little difference between modulus of elasticity values measured by nanoindentation in air or liquid. This hypothesis is verified by Peakforce QNM measurements on the same α-synuclein fibrils in air and liquid, which did not result in significant differences [56].

For bending rigidity measurements from topography images, the surrounding medium will influence the interaction of the fibrils with the surface. This interaction will determine whether the fibrils on the surface are thermally equilibrated or whether they are irreversibly trapped. More specifically the ion concentration determines the strength of this interaction. When imaging DNA in solution the Mg2+ ion concentration is responsible for the ability of DNA to move on the surface. This ability to move is important to make sure that the sample is in thermal equilibrium for persistence length analyses [79]. However, in the case of amyloid fibrils with their strong adhesive properties this is difficult. Several studies claim that amyloid fibrils are in thermal equilibrium on the surface (often mica surfaces) [51, 53]. A study on HypF-*N* fibrils also indicated that the fibrils equilibrate after deposition on mica [69]. Recent work on bending rigidity analysis of alpha-synuclein fibrils on fluid phase lipid membranes compared to the same fibrils on mica supports these claims. The fibrils did not strongly bind to the membrane and were still able to move around, clearly suggesting that they are thermally equilibrated on the surface when imaged. Mechanical analyses did not show differences in bending rigidity values between the fibrils on mica and the loosely bound fibrils on the membrane [80]. Also, imaging amyloid fibrils in ambient air environment did not give different bending rigidity values compared to fibrils imaged in solution [62].

4. Towards higher ordered structures

The increasing interest in mechanical properties of amyloid fibrils is summarized in figure 6, from a recent article by Knowles and Buehler [81]. This figure collates all available values of bending rigidities and moduli of elasticity of amyloid and compares these mechanical characteristics to other biological and non-biological materials. As shown in panel (B) the range of modulus of elasticity values found for amyloid fibrils is rather large. This is most likely attributable to the different approaches used to calculate these values, and reflects, for instance, the anisotropic differences that are shown by nanoindentation and bending measurements (section 3.3). Also, polymorphism results in differences in elastic moduli due to different conformations within the fibrils leading to different moments of inertia (section 3.2). The bending rigidities depicted in panel (A) are experimentally less susceptible to calibration errors and small size issues. It is most instructive to compare bending rigidities of amyloids to other biological structures in their native form. Mechanical characteristics of amyloid could lead to new insights in disease-related processes, for instance by directly relating the mechanical properties of amyloid to cytoskeleton properties. However, the nanomechanical properties of amyloids are also related to amyloid growth kinetics. It has been suggested that longer fibrils have a greater propensity towards fracture [82, 83]. This creates

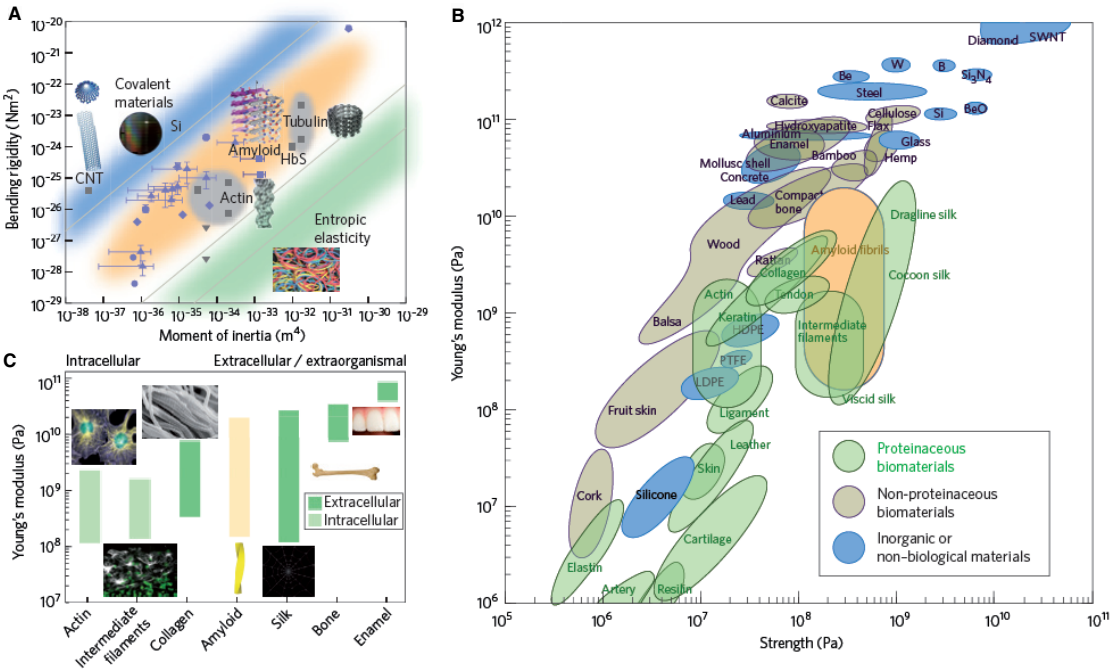

Figure 6. Mechanical properties of amyloid fibrils in comparison to biological and inorganic or non-biological materials. Panel (A) shows bending rigidities versus moments of inertia for materials with covalent bonds (blue region), non-covalent bonds such as hydrogen bonds (orange region) and weak non-covalent interactions (green region). Blue and gray symbols are values for different types of amyloid fibrils measured experimental or from simulations. Panel (B) indicates modulus of elasticity versus strength for different types of materials. Panel (C) represents different modulus of elasticity ranges for different classes of biological materials. Reproduced with permission from [81]. Copyright 2011 Nature Publishing Group.

more fibril ends increasing the overall aggregation reaction by generating new growth sites due to fragmentation [84]. The Knowles group has treated in a comprehensive theoretical manner, the issue of nucleated polymerization with secondary pathways [85–87]. An experimental study has demonstrated that prion protein fibrils with a lower fracture rate can lose their ability to propagate as prions [88]. However, prion fibrils with a high propensity towards fracture propagate more effectively, and could result in a more rapid onset of disease symptoms.

Furthermore, mechanical characteristics in the form of moduli of elasticity or stiffness are useful to investigate the use of amyloid fibrils for nanomaterials, especially for construction of larger, more complex, supramolecular assemblies.

The propensity of protein peptides to self-assemble into amyloid fibrils crosses over into self-assembly of fibrils into higher ordered structures such as gels, crystals or films. The mechanical properties of these higher ordered assemblies depend on the mechanical properties of the single amyloid fibrils as well as on the packing density, packing structure, and cross linking of these fibrils or proteins within the structure. Insulin crystals display a modulus of elasticity measured with nanoindentation of 164 MPa, a value that is almost ten-fold lower compared to the nanoindentation results on single insulin fibrils [57, 89]. Gels formed with insulin fibrils show moduli ranging from 4 Pa to above 20 Pa depending on concentration and the aggregation kinetics [90]. Gels formed with TSS1 fibrils (three-stranded β-sheet) show storage moduli of 2–9 kPa depending on the pH in which the gels are formed [91]. The tunable mechanical properties of the (hydro)-gels mentioned above make these structures even more interesting for usage in tissue regeneration. Studies with collagen films with different mechanical properties already show that muscle cells spread and proliferate more extensively on softer collagen fibrils compared to stiffer fibrils where the cells hardly show movement [92]. The mechanical properties of the underlying substrate influence not only movement and growth of cells, but are also reported to affect the differentiation of stem cells. Naive mesenchymal stem cells have been shown to differentiate towards neuronal cells when cultured on scaffolds mimicking the mechanical properties of brain tissue, whereas when cultured on stiffer collagenous bone-like scaffolds they become osteogenic [93]. A few studies report the use of amyloid as scaffolds for tissue regeneration purposes [94, 95]. A scaffold made of peptide nanofibers seemed to regenerate axons and knit brain tissue together, leading to functional return of vision in small mammals after completely severing the optic tract [94].

5. Concluding remarks

Measuring and understanding the mechanical characteristics of single amyloid fibrils could thus give insight into many different biological contexts. For the disease-related amyloids, these mechanical properties may shed light on the pathology and mechanism of the disease. Functional amyloids often have remarkable mechanical properties, for instance natural

adhesive amyloids, which could be exploited for newly developed biological adhesives. Furthermore, amyloids are already proven to be useful in constructing functionalized nanowires or in larger network-type materials. Tuning the mechanical properties of amyloid-based nanostructures thus offers the potential for further functional applications of amyloids as novel nanobiomaterials.

References

[1] Sipe J D and Cohen A S 2000 Review: history of the amyloid fibril *J. Struct. Biol.* **130** 88–98

[2] Dobson C M 2003 Protein folding and misfolding *Nature* **426** 884–90

[3] Chiti F and Dobson C M 2006 Protein misfolding, functional amyloid and human disease *Annu. Rev. Biochem.* **75** 333–66

[4] Fowler D M, Koulov A V, Balch W E and Kelly J W 2007 Functional amyloid—from bacteria to humans *Trends Biochem. Sci.* **32** 217–24

[5] Sagis L M C, Veerman C and van der Linden E 2004 Mesoscopic properties of semiflexible amyloid fibrils *Langmuir* **20** 924–7

[6] Kroes-Nijboer A, Venema P and van der Linden E 2012 Fibrillar structures in food *Food Funct.* **3** 221–27

[7] Nelson R, Sawaya M R, Balbirnie M, Madsen A Ø, Riekel C, Grothe R and Eisenberg D 2005 Structure of the cross-β spine of amyloid fibrils *Nature* **435** 773–8

[8] Ban T, Hamada D, Hasegawa K, Naiki H and Goto Y 2003 Direct observation of amyloid fibril growth by thioflavin T fluorescence *J. Biol. Chem.* **278** 16462–5

[9] Sunde M, Serpell L C, Bartlam M, Fraser P E, Pepys M B and Blake C C F 1997 Common core structure of amyloid fibrils by synchrotron x-ray diffraction *J. Mol. Biol.* **273** 729–39

[10] Cherny I and Gazit E 2008 Amyloids: not only pathological agents but also ordered nanomaterials *Angew. Chem. Int. Edn Engl.* **47** 4062–9

[11] Petkova A T, Leapman R D, Guo Z, Yau W, Mattson M P and Tycko R 2005 Self-propagating, molecular-level polymorphism in Alzheimer's β-amyloid fibrils *Science* **307** 262–5

[12] Adamcik J and Mezzenga R 2011 Adjustable twisting periodic pitch of amyloid fibrils *Soft Matter* **7** 5437–43

[13] Vilar M, Chou H, Luhrs T, Maji S K, Riek-Loher D, Verel R, Manning G, Stahlberg H and Riek R 2007 The fold of α-synuclein fibrils *Proc. Natl Acad. Sci.* **105** 8637–42

[14] Heise H, Hoyer W, Becker S, Andronesi O C, Riedel D and Baldus M 2005 Molecular-level secondary structure, polymorphism, and dynamics of full-length α-synuclein fibrils studied by solid-state NMR *Proc. Natl Acad. Sci.* **102** 15871–6

[15] Gosal W S, Myers S L, Radford S E and Thomson N H 2006 Amyloid under the atomic force microscope *Protein Pep. Lett.* **13** 261–70

[16] Fändrich M, Meinhardt J and Grigorieff N 2009 Structural polymorphism of Alzheimer Aβ and other amyloid fibrils *Prion* **3** 89–93

[17] Kodali R and Wetzel R 2007 Polymorphism in the intermediates and products of amyloid assembly *Curr. Opin. Struct. Biol.* **17** 48–57

[18] Kumar S and Udgaonkar J B 2010 Mechanisms of amyloid fibril formation by proteins *Curr. Sci.* **98** 639–56

[19] Kojima H, Ishijima A and Yanagida T 1994 Direct measurement of stiffness of single actin filaments with and without tropomyosin by in vitro nanomanipulation *Proc. Natl Acad. Sci.* **91** 12962–6

[20] Claessens M M A E, Bathe M, Frey E and Bausch A R 2006 Actin-binding proteins sensitively mediate F-actin bundle stiffness *Nature Mater.* **5** 748–53

[21] Van Buren V, Cassimeris L and Odde D J 2005 Mechanochemical model of microtubule structure and self-assembly kinetics *Biophys. J.* **89** 2911–26

[22] Schaap I A T, Carrasco C, de Pablo P J, Mackintosh F C and Schmidt C F 2006 Elastic response, buckling, and instability of microtubules under radial indentation *Biophys. J.* **91** 1521–31

[23] Fudge D S, Gardner K H, Forsyth V T, Riekel C and Gosline J M 2003 The mechanical properties of hydrated intermediate filaments: insights from hagfish slime threads *Biophys. J.* **85** 2015–27

[24] Yang L, van der Werf K O, Koopman B F J M, Subramaniam V, Bennink M L, Dijkstra P J and Feijen J 2007 Micromechanical bending of single collagen fibrils using atomic force microscopy *J. Biomed. Mater. Res.* **82** 160–8

[25] Heim A J and Matthews W G 2006 Determination of the elastic modulus of native collagen fibrils via radial indentation *Appl. Phys. Lett.* **89** 181902

[26] Maji S K *et al* 2009 Functional amyloids as natural storage of peptide hormones in pituitary secretory granules *Science* **325** 328

[27] Maji S K, Schubert D, Rivier C, Lee S, Rivier J E and Riek R 2008 Amyloid as a depot for the formulation of long-acting drugs *PLoS Biol.* **6** e17

[28] Mostaert A S, Higgins M J, Fukuma T, Rindi F and Jarvis S P 2006 Nanoscale mechanical characterization of amyloid fibrils discovered in a natural adhesive *J. Biol. Phys.* **32** 393–401

[29] Barnhart M M and Chapman M R 2006 Curli biogenesis and function *Annu. Rev. Microbiol.* **60** 131–47

[30] Sullan R M A, Gunari N, Tanur A E, Chan Y, Dickinson G H, Orihuela B, Rittschof D and Walker G C 2009 Nanoscale structures and mechanics of barnacle cement *Biofouling* **253** 263–75

[31] Scheibel T, Parthasarathy R, Sawicki G, Lin X, Jeager H and Lindquist S L 2003 Conducting nanowires built by controlled self-assembly of amyloid fibers and selective metal deposition *Proc. Natl Acad. Sci.* **100** 4527–32

[32] Carny O, Shalev D and Gazit E 2006 Fabrication of coaxial metal nanocables using a self-assembled peptide nanotube scaffold *Nano Lett.* **6** 1594–7

[33] Binnig G and Rohrer H 2000 Scanning tunneling microscopy (reprinted from 1986) *IBM J. Res. Dev.* **44** 279–93

[34] Binnig G and Quate C F 1986 Atomic force microscope *Phys. Rev. Lett.* **56** 930–3

[35] Hoh J H and Engel A 1993 Friction effects on force measurements with an atomic force microscope *Langmuir* **9** 3310–2

[36] Hertz H 1881 Über die Berührung fester elastischer Körper (on the contact of elastic solids) *J. Reine Angew. Math.* **92** 156–71

[37] Derjaguin B V, Muller V M and Toporov Y U P 1975 Effect of contact deformations on the adhesion of particles *J. Colloid Interface Sci.* **53** 2

[38] Johnson K L, Kendall K and Roberts A D 1971 Surface energy and the contact of elastic solids *Proc. R. Soc.* A **324** 301–13

[39] Van der Werf K O, Putman C A J, de Grooth B G and Greve J 1994 Adhesion force imaging in air and liquid by adhesion mode atomic force microscopy *Appl. Phys. Lett.* **65** 1195–7

[40] Pittenger B, Erina N and Su C 2010 *Quantitative Mechanical Property Mapping at the Nanoscale with Peakforce QNM Application Note* (Santa Barbara, CA: Veeco Instruments Inc.)

[41] Rosa-Zeiser A, Weilandt E, Hild S and Marti O 1997 The simultaneous measurement of elastic, electrostatic and adhesive properties by scanning force microscopy: pulsed-force mode operation *Meas. Sci. Technol.* **8** 1333–8

[42] Sahin O 2007 Harnessing bifurcations in tapping-mode atomic force microscopy to calibrate time-varying tip–sample force measurements *Rev. Sci. Instrum.* **78** 103707

[43] Garcia V J, Martinez L, Briceno-Valero J M and Schilling C H 1997 Dimensional metrology of nanometric spherical particles using AFM: II, application of model-tapping mode *Probe Microsc.* **1** 107–16

[44] Burnham N A, Behrend O P, Oulevey F, Germaud G, Gallo P J, Gourdon D, Dupas E, Kulik A J, Pollok H M and Briggs G A D 1997 How does a tip tap *Nanotechnology* **8** 67–75

[45] Borgia A, Williams P M and Clarke J 2008 Single-molecule studies of protein folding *Annu. Rev. Biochem.* **77** 101–25

[46] Puchner E M and Gaub H E 2009 Force and function: probing proteins with AFM-based force spectroscopy *Curr. Opin. Struct. Biol.* **19** 605–14

[47] Fukuma T, Mostaert A S and Jarvis S P 2006 Explanation for the mechanical strength of amyloid fibrils *Tribol. Lett.* **22** 233–7

[48] Kjelstrup-Hansen J, Hansen O, Rubhan H G and Bøggild P 2006 Mechanical properties of organic nanofibers *Small* **2** 660–6

[49] Koenders M M J F, Yang L, Wismans R G, Van der Werf K O, Reinhardt D P, Daamen W, Bennink M L, Dijkstra P J, Van Kuppevelt T H and Feijen J 2009 Microscale mechanical properties of single elastic fibers: the role of fibrillin-microfibrils *Biomaterials* **30** 2425–32

[50] Howard J 2001 *Mechanics of Motor Proteins and the Cytoskeleton* (Sunderland, MA: Sinauer Associates)

[51] Knowles T P, Fitzpatrick A W, Meehan S, Mott H R, Vendruscolo M, Dobson C M and Welland M E 2007 Role of intermolecular forces in defining material properties of protein nanofibrils *Science* **318** 1900–3

[52] Wang J C, Turner M S, Agarwal G, Kwong S, Josephs R, Ferrone F A and Briehl R W 2002 Micromechanics of isolated sickle cell hemoglobin fibers: bending moduli and persistence lengths *J. Mol. Biol.* **315** 601–12

[53] Smith J F, Knowles T P J, Dobson C M, MacPhee C M and Welland M E 2006 Characterization of the nanoscale properties of individual amyloid fibrils *Proc. Natl Acad. Sci.* **103** 15806–11

[54] Ohler B 2007 Cantilever spring constant calibration using laser Doppler vibrometry *Rev. Sci. Instrum.* **78** 063107

[55] Cook S M, Schäffer T E, Chynoweth K M, Wigton M, Simmonds R W and Lang K M 2006 Practical implementation of dynamic methods for measuring atomic force microscope cantilever spring constants *Nanotechnology* **17** 2135–45

[56] Gibson C T, Smith D A and Roberts C J 2005 Calibration of silicon atomic force microscope cantilevers *Nanotechnology* **16** 234–8

[57] Akhremitchev B B and Walker G C 1999 Finite sample thickness effects on elasticity determination using atomic force microscopy *Langmuir* **15** 5630–4

[58] Guo S and Akhremitchev B B 2006 Packing density and structural heterogeneity of insulin amyloid fibrils measured by afm nanoindentation *Biomacromolecules* **7** 1630–6

[59] Mercato del L L, Maruccio G, Pompa P P, Bochicchio B, Tamburro A M, Cingolani R and Rinaldi R 2008 Amyloid-like fibrils in elastin-related polypeptides: structural characterization and elastic properties *Biomacromolecules* **9** 796–803

[60] Khurana R, Ionescu-Zanetti C, Pope M, Li J, Nielson L, Ramirez-Alvarado M, Regan L, Fink A L and Carter S A 2003 A general model for amyloid fibril assembly based on morphological studies using atomic force microscopy *Biophys. J.* **85** 1135–44

[61] Adamcik J, Jung J, Flakowski J, De Los Rios P, Dietler G and Mezzenga R 2010 Understanding amyloid aggregation by statistical analysis of atomic force microscopy images *Nature Nanotechnol.* **5** 423–8

[62] Sweers K K M, Segers-Nolten N J M, Bennink M L and Subramaniam V 2012 Structural model for α-synuclein fibrils derived from high resolution imaging and nanomechanical studies using atomic force microscopy *Soft Matter* at press

[63] Makin O and Serpell L C 2005 Structures for amyloid fibrils *FEBS J.* **272** 5959–61

[64] Karsai Á, Mártonfalvi Z S, Nagy A, Grama L, Penke B and Kellermayer M S Z 2006 Mechanical manipulation of alzheimer's amyloid β1–42 fibrils *J. Struct. Biol.* **155** 316–26

[65] Kellermayer M S Z, Grama L, Karsai Á, Nagy A, Kahn A, Datki Z L and Penke B 2005 Reversible mechanical unzipping of amyloid β-fibrils *J. Biol. Chem.* **290** 8464–70

[66] Bhak G, Lee S, Park J W, Cho S and Paik S R 2010 Amyloid hydrogel derived from curly protein fibrils of α-synuclein *Biomaterials* **31** 5986–95

[67] Jordens S, Adamcik J, Amar-Yuli I and Mezzenga R 2011 Disassembly and reassembly of amyloid fibrils in water-ethanol mixtures *Biomacromolecules* **12** 187–93

[68] Dunstan D E, Hamilton-Brown P, Asimakis P, Ducker W and Bertolini J 2009 Shear-induced structure and mechanics of β-lactoglobulin amyloid fibrils *Soft Matter* **5** 5020–8

[69] Relini A, Torrassa S, Ferrando R, Rolandi R, Campioni S, Chiti F and Gliozzi A 2010 Detection of populations of amyloid-like protofibrils with different physical properties *Biophys. J.* **98** 1277–84

[70] Minary-Jolandan M and Yu M 2009 Nanomechanical heterogeneity in the gap and overlap regions of type I collagen fibrils with implications for bone heterogeneity *Biomacromolecules* **10** 2565–70

[71] Segers-Nolten I, Van der Werf K, Van Raaij M and Subramaniam V 2007 Quantitative characterization of protein nanostructures using atomic force microscopy *Proc. IEEE Conf. Eng. Med. Biol. Soc.* pp 6609–12

[72] Zhou X, Cui C Y, Zhang J, Liu J and Liu J 2010 Nanomechanics of individual amyloid fibrils using atomic force microscopy *Chin. Sci. Bull.* **55** 1608–12

[73] Adamcik J, Berquand A and Mezzenga R 2011 Single-step direct measurement of amyloid fibrils stiffness by peak force quantitative nanomechanical atomic force microscopy *Appl. Phys. Lett.* **98** 193701

[74] Kol N, Adler-Abramovich L, Barlam D, Shneck R Z, Gazit E and Rousso I 2005 Self-assembled peptide nanotubes are uniquely rigid bioinspired supramolecular structures *Nano Lett.* **5** 1343–6

[75] Niu L J, Chen X Y, Allen S and Tendler S J B 2007 Using the bending beam model to estimate the elasticity of diphenylalanine nanotubes *Langmuir* **23** 7443–6

[76] Flamia R, Zhdan P A, Castle J E and Tamburro A M 2008 Comment on the mechanical properties of the amyloid fibre, poly(ValGlyGlyLeuGly), obtained by a novel AFM methodology *J. Mater. Sci.* **43** 395–7

[77] Moreno-Herrero F, Perez M, Baro A M and Avila J 2004 Characterization by atomic force microscopy of alzheimer paired helical filaments under physiological conditions *Biophys. J.* **86** 517–25

[78] Verhoff T, Glišović A, Schollmeyer H, Zippelius A and Salditt T 2007 Mechanical properties of spider dragline silk: humidity, hysteresis and relaxation *Biophys. J.* **93** 4425–32

[79] Mücke N, Kreplak L, Kirmse R, Wedig T, Herrmann H, Aebi U and Langowski J 2004 Assessing the flexibility of intermediate filaments by atomic force microscopy *J. Mol. Biol.* **335** 1241–50

[80] Sweers K K M, Bennink M L and Subramaniam V 2012 Alpha-synuclein fibril interaction with supported lipid billayers investigated with atomic force microscopy, in preparation
[81] Knowles T P J and Beuhler M J 2011 Nanomechanics of functional and pathological amyloid materials *Nature Nanotechnol.* **6** 469–79
[82] Shorter J and Lindquist S 2006 Destruction of potentiation of different prions catalyzed by similar Hsp 104 remodeling activities *Mol. Cell* **23** 425–38
[83] Paparcone R and Buehler M J 2011 Failure of A-beta-(1–40) amyloid fibrils under tensile loading *Biomaterials* **32** 3367–74
[84] Cohen S I A, Vendruscolo M, Dobson C M and Knowles T P J 2011 Nucleated polymerization in the presence of pre-formed seed filaments *Int. J. Mol. Sci.* **12** 5844–52
[85] Cohen S I A, Vendruscolo M, Welland M E, Dobson C M, Terentjev E M and Knowles T P J 2011 Nucleated polymerization with secondary pathways. I. Time evolution of the principal moments *J. Chem. Phys.* **135** 065105
[86] Cohen S I A, Vendruscolo M, Dobson C M and Knowles T P J 2011 Nucleated polymerization with secondary pathways. II. Determination of self-consistent solutions to growth processes described by non-linear master equations *J. Chem. Phys.* **135** 065106
[87] Cohen S I A, Vendruscolo M, Dobson C M and Knowles T P J 2011 Nucleated polymerization with secondary pathways. III. Equilibrium behavior and oligomer populations *J. Chem. Phys.* **135** 065107
[88] Wang Y, Buell A K, Wang X, Welland M E, Dobson C M, Knowles T P J and Perret S 2011 Relationship between prion propensities and the rates of individual molecular steps of fibril assembly *J. Biol. Chem.* **286** 12101–7
[89] Guo S and Akhremitchev B B 2008 Investigation of mechanical properties of insulin crystals by atomic force microscopy *Langmuir* **24** 880–7
[90] Manno M, Giacomazza D, Newman J, Martorana V and San Biagio P L 2010 Amyloid gels: precocious appearance of elastic properties during the formation of an insulin fibrillar network *Langmuir Lett.* **26** 1424–6
[91] Rughani R V, Salick D A, Lamm M S, Yucel T, Pochan D J and Schneider J P 2009 Folding, self-assembly, and bulk material properties of a de novo designed three-stranded β-sheet hydrogel *Biomacromolecules* **10** 1295–304
[92] McDaniel D P, Shaw G A, Elliott J T, Bhadriraju K, Meuse C, Chung K and Plant A L 2007 The stiffness of collagen fibrils influences vascular smooth muscle cell phenotype *Biophys. J.* **92** 1759–69
[93] Engler A J, Sen S, Sweeney H L and Discher D E 2006 Matrix elasticity directs stem cell lineage specification *Cell* **126** 677–89
[94] Ellis-Behnke R G, Liang Y, You S, Tay D K C, Zhang S, So K and Schneider G E 2006 Nano neuro knitting: peptide nanofiber scaffold for brain repair and axon regeneration with functional return of vision *Proc. Natl Acad. Sci.* **28** 5054–9
[95] Holmes T C, De Lacalle S, Su X, Liu G, Rich A and Zhang S 2000 Extensive neurite outgrowth and active synapse formation on self-assembling peptide scaffolds *Prot. Natl Acad. Sci.* **97** 6728–33